Review of Scientific Instruments

Time-of-flight spectrometry of ultra-short, polyenergetic proton bunches

Cite as: Rev. Sci. Instrum. **89**, 123302 (2018); https://doi.org/10.1063/1.5052059
Submitted: 14 August 2018 . Accepted: 26 November 2018 . Published Online: 13 December 2018

Matthias Würl, Franz S. Englbrecht, Sebastian Lehrack, Chiara Gianoli, Florian H. Lindner, Thomas F. Rösch, Daniel Haffa, Francesco Olivari, Marco Petasecca, Michael L. F. Lerch, Alexandre Pogossov, Linh T. Tran, Walter Assmann, Jörg Schreiber, Anatoly B. Rosenfeld, and Katia Parodi

Time-of-flight spectrometry of ultra-short, polyenergetic proton bunches

Matthias Würl,[1] Franz S. Englbrecht,[1] Sebastian Lehrack,[1] Chiara Gianoli,[1] Florian H. Lindner,[1] Thomas F. Rösch,[1] Daniel Haffa,[1] Francesco Olivari,[1,2] Marco Petasecca,[3] Michael L. F. Lerch,[3] Alexandre Pogossov,[3] Linh T. Tran,[3] Walter Assmann,[1] Jörg Schreiber,[1,4] Anatoly B. Rosenfeld,[3] and Katia Parodi[1]
[1]*Department of Medical Physics, Faculty of Physics, Ludwig-Maximilians-Universität München, 85748 Garching, Germany*
[2]*Dipartimento di Fisica, Università degli studi di Pavia, 27100 Pavia, Italy*
[3]*Centre for Medical Radiation Physics, University of Wollongong, Wollongong, NSW 2522, Australia*
[4]*Max-Planck-Institut für Quantenoptik, 85748 Garching, Germany*

(Received 14 August 2018; accepted 26 November 2018; published online 13 December 2018)

A common approach for spectrum determination of polyenergetic proton bunches from laser-ion acceleration experiments is based on the time-of-flight (TOF) method. However, spectra obtained using this method are typically given in relative units or are estimated based on some prior assumptions on the energy distribution of the accelerated ions. In this work, we present a new approach using the TOF method that allows for an absolute energy spectrum reconstruction from a current signal acquired with a sub-nanosecond fast and 10 μm thin silicon detector. The reconstruction is based on solving a linear least-squares problem, taking into account the response function of the detection system. The general principle of signal generation and spectrum reconstruction by setting up an appropriate system response matrix is presented. Proof-of-principle experiments at a 12 MV Tandem accelerator using different nanosecond-short (quasi-)monoenergetic and polyenergetic proton bunches at energies up to 20 MeV were successfully performed. Within the experimental uncertainties of 2.4% and 12.1% for energy and particle number, respectively, reconstructed energy distributions were found in excellent agreement with the spectra calculated using Monte Carlo simulations and measured by a magnetic spectrometer. This TOF method can hence be used for absolute online spectrometry of laser-accelerated particle bunches. *Published by AIP Publishing.* https://doi.org/10.1063/1.5052059

I. INTRODUCTION

Upcoming laboratories housing petawatt laser systems operating at high repetition rates are pushing laser-driven ion acceleration further towards applications ranging also beyond fundamental research, e.g., biomedical applications.[1] In Garching near Munich, the Centre for Advanced Laser Applications (CALA) equipped with the ATLAS-3000 laser system is close to starting operation. This Ti:sapphire based laser system will provide 60 J pulse energy within a pulse duration of 20 fs at a repetition rate of 1 Hz. Planned research is directed towards laser-driven ion bunch radiotherapy (LIBRT) and the fission-fusion reaction mechanism.[2]

The special features of laser-driven ion sources are a mixed radiation field of different ion species at different charge states, relativistic electrons and electromagnetic radiation, a small source size ($\sim\mu$m) and divergence angles up to a few tens of degrees, and short emission times ($\lesssim$ps) and broad energy distributions ($\sim$100%), combined with a tremendous number of particles ($\sim 10^9$–10^{10} protons/bunch).[1–4] Proton energies approaching 100 MeV have recently been reported.[5] Great effort is being devoted to develop devices capable of focusing and guiding the highly divergent ion bunches towards application sites.[6–9]

Knowledge of the absolute particle number per energy per unit area is requisite for most applications. Due to shot-to-shot fluctuations in the energy spectrum, an online and non-destructive characterization of each individual ion bunch, ideally in transmission and close to the application, is desirable. Although characterization of laser-accelerated ion (LION) bunches by time-of-flight (TOF) measurements utilizing ion collectors or plastic scintillators has already been done more than a decade ago,[10,11] this method is becoming increasingly popular in the community with developments in novel solid state detectors.[12–14] Ion spectra retrieved by the TOF method are typically given in arbitrary units[7,15,16] and/or are based on assumptions on the energy distributions of different ions at different charge states.[14,17] However, these kind of assumptions are no longer valid when passive or active beam shaping devices like permanent magnetic quadrupoles, solenoids, or plasma focusing are applied.

In this paper, we therefore present a novel and simple approach for absolute TOF spectrometry of ultra-short, polychromatic proton bunches—the typically most dominant ion species in laser-ion acceleration experiments due to the highest charge-to-mass ratio. The method is based on extracting the spectral information from the pile-up current signal, generated by the polychromatic ion bunch inside a novel fast silicon detector while taking into account the response function of the entire detection system. The approach is complemented by proof-of-principle measurements performed at a 12 MV Tandem accelerator, providing well-controlled and reproducible conditions. (Quasi-)monoenergetic and polyenergetic, ns-short proton bunches with kinetic energies up to 20 MeV were obtained using dedicated passive absorbers. Reconstructed energy distributions are compared to

measurements using a magnetic spectrometer and to FLUKA Monte Carlo (MC) simulations.[18,19]

II. MATERIALS AND METHODS

A. Reconstruction of polychromatic proton energy distributions

1. Considerations for the spectrum reconstruction

When measuring the TOF signal of short and intense bunches, as generated in laser-ion acceleration, the detector is exposed to a few nanosecond short and continuous irradiation starting from the highest energetic protons to the slowest protons that can still enter the sensitive volume (SV) of the detector. Due to the high fluxes, it is not possible to distinguish between individual particles. Hence, the measured signal is the pile-up of numerous individual events. Resolving the signal components generated by individual particles by means of deconvolution or pulse fitting, like performed in, e.g., Marrone *et al.*[20] and Belli *et al.*,[21] becomes virtually impossible. However, a deconvolution approach would become feasible if the continuous ion bunch was considered as being composed of many short particle sub-bunches, where each sub-bunch contains all particles arriving at the detector within a certain time interval Δt.

After discretizing the continuous signal, which is inherently done by digitizing the analog detector signal, the measured signal can thus be treated as a superposition of many signals each generated by an individual proton sub-bunch with a duration of the digitizer's sampling width. Given a source-detector drift length d and assuring that at $t = 0$ all particles start to drift simultaneously, every time bin around a sampling point t_{TOF} corresponds to a discrete energy window around its corresponding central energy

$$E_{kin}(t_{\mathrm{TOF}}) = \left(\frac{1}{\sqrt{1 - \left(\frac{d}{c \cdot t_{\mathrm{TOF}}}\right)^2}} - 1 \right) \cdot m_p c^2, \qquad (1)$$

where c and m_p are the speed of light and the proton rest mass, respectively.

In case of LIONs, the starting time t_0 is given by the electromagnetic pulse and ultra-relativistic electrons that are co-emitted from the plasma and reach the detector at $t_{\gamma,e} \approx d/c$. Additionally, the use of an external trigger signal closely correlated to t_0 is beneficial. This could be for instance a fast photodiode detecting the fraction of the main laser pulse that is transmitted through one of the mirrors in the laser beamline. Of course, this trigger needs to be thoroughly synchronized with the actual arrival of the laser pulse at the laser-plasma interaction point.

Ion velocities in contemporary laser-based ion acceleration experiments are typically in the (near-)relativistic range, reaching values up to ~0.4c. Having a reasonable drift space of a few meters, this translates to drift times in the order of some nanoseconds. For instance, the TOF difference of protons with energies of 49 MeV and 50 MeV is 0.1 ns per meter drift length. This implies that the finite response function of the detector and successive electronics has to be taken into account when reconstructing an energy spectrum from the measured TOF signals. It is also worthwhile to mention that a proper cable selection with low damping at high frequencies is crucial for TOF spectrometry in these ion energy ranges.

Since the measured TOF signal can be treated as a superposition of signals generated by discrete ion sub-bunches with a given energy bin width $\Delta E_{kin}(t_{\mathrm{TOF}})$, the ion spectrum can be obtained by solving a regularized linear least-squares problem

$$\min \|\mathcal{A}\vec{x} - \vec{S}\|^2 + \|L_\mu \vec{x}\|^2, \quad x_i \geq 0 \; \forall i, \qquad (2)$$

with the constraint that all reconstructed particle numbers x_i in every energy bin i must be positive. The vector $\vec{S}$ is the digitized TOF signal and $\mathcal{A}$ is the system response matrix. Since the inverse problem to be solved is ill-posed and the solution is expected to be rather smooth, Tikhonov regularization[22] was used to penalize overfitting at the cost of a broadening of the reconstructed energy spectrum. The regularization matrix $L_\mu = \mu\mathbb{I}$ is composed of the regularization parameter $\mu > 0$ and the identity matrix $\mathbb{I}$. In order to find an adequate solution to the inverse problem, μ is determined empirically according to the measured signal. For $\mu = 0$, the equation becomes the unregularized least-squares problem.

2. Generation of the system response matrix

The system matrix $\mathcal{A}$ needs to account for the response function of the detector and electronics, as well as the initial temporal structure of the proton bunch. For laser-ion acceleration, this initial temporal bunch structure can be considered as a delta function and can hence be neglected. If the bunch duration is of comparable length as the detector response function, it has to be taken into account for creating $\mathcal{A}$. For the proof-of-principle experiments at the Tandem accelerator presented in this work, this initial temporal bunch structure was therefore included in the system response matrix.

Two approaches to obtain the response function of the detector and the successive electronics were performed in this study. First, the detector was irradiated with nanosecond-short monoenergetic proton bunches from the Tandem accelerator, which we also used for the TOF measurements presented hereafter. In that case, the measured response is actually the convolution of the detector response function and the temporal shape of the short proton bunches. The measured response at the Tandem accelerator, normalized by the energy deposition inside the SV of the detector, is shown in the inset of Fig. 1.

A different way to obtain the response function itself is by exposing the detector to an ultra-short (<1 ps) laser pulse,

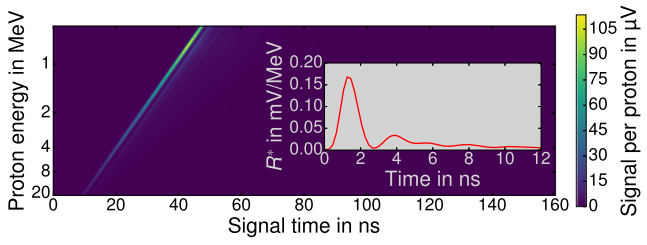

FIG. 1. Graphical representation of the system response matrix created for the TOF experiments at the Tandem accelerator ($d = 52$ cm). The colors represent the expected signal amplitude per proton within a certain energy bin. The inset shows the normalized detector response function $R^*(t)$.

given that the used detector is sensitive to the wavelength of the laser light. We used a femtosecond Ti:sapphire laser system (CentAurus X, Amplitude Technologies, France) with a central wavelength of 800 nm and attenuated the pulse energy using absorptive filters. At this wavelength, energy absorption is expected to be almost uniform within the 10 μm thin silicon SV of the used detector and can hence be assumed to be similar to ion irradiation. The response R_{meas} was measured for different laser light intensities. Linearity of the response with laser intensity was obtained for signal amplitudes relevant in the presented experiments.

To obtain an absolute particle number calibration, this measured response R_{meas} (with or without temporal structure of the proton bunch) is then normalized by the energy deposition in the SV of the detector according to

$$R^* = \frac{R_{\mathrm{meas}}}{N_{\mathrm{p}}^{\mathrm{SV}} \cdot \left\langle E_{\mathrm{dep}}(E_{\mathrm{kin}}) \right\rangle}, \tag{3}$$

where $N_{\mathrm{p}}^{\mathrm{SV}}$ is the number of protons reaching the detector's SV and $\left\langle E_{\mathrm{dep}}(E_{\mathrm{kin}}) \right\rangle$ is the average energy deposition in the SV by one proton of the kinetic energy used for the calibration (E_{kin} = 20 MeV). The proton number is based on offline beam current measurements using a Faraday cup (FC) when recording the response function. An estimation of the particle fraction reaching the detector's SV was taken from FLUKA MC simulations including the detector geometry and measured beam spot size. The average energy deposition in the detector, $\left\langle E_{\mathrm{dep}}(E_{\mathrm{kin}}) \right\rangle$, was also taken from simulations.

A graphical representation of the system response matrix used for our experiments at the Tandem accelerator is shown in Fig. 1. The system matrix was created by inserting copies of the normalized response R^* along the second dimension (rows), where each copy is successively shifted one sampling point by inserting a zero at the beginning of the response array. The copies are scaled in amplitude according to the mean energy deposition inside the SV by protons with energies corresponding to that time sampling point (Fig. 2). Thus, every row in the matrix corresponds to the expected detector signal

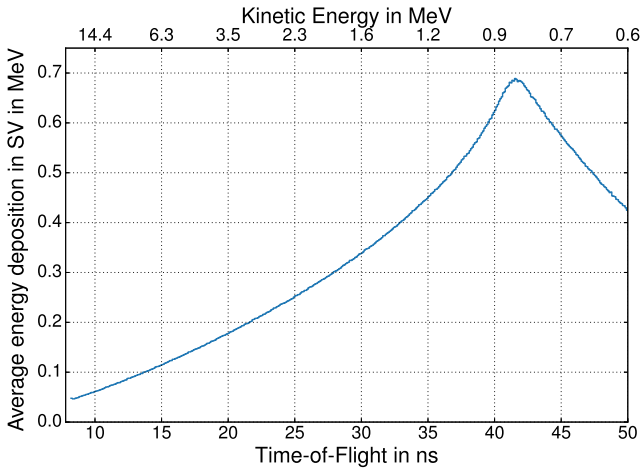

FIG. 2. MC calculated average energy deposition in the 10 μm thin sensitive volume (SV) of the detector, depending on the kinetic energy of the protons and the corresponding time-of-flight for d = 52 cm. From the observed peak towards lower energies, protons stop within the SV.

generated by one proton reaching the detector within a given time window. The same cable type and length was taken for measurement of the response function and for the actual TOF measurements, since the shape of the response function may be affected by damping of high frequency components in the cables.

B. TOF measurements at the MLL Tandem accelerator

In order to test the spectrum determination under controlled and reproducible conditions, first proof-of-principle experiments were performed at the MLL Tandem accelerator[23] with 20 MeV protons. Bunches with a duration of around 1 ns were obtained using the built-in chopper and buncher system.[24] The average beam current was (0.8 ± 0.2) nA. From the 5 MHz chopper frequency, we reduced the pulse repetition rate down to 9765 bunches per second due to limitations of the used data acquisition system. The number of protons per bunch was hence (5.1 ± 1.3) × 10^5.

1. Overview of the experimental setup

A schematic overview of the experimental setup can be seen in Fig. 3. The entire experiment was performed in vacuum. For practical reasons, the main vacuum chamber was separated from the accelerator beamline vacuum by a 50 μm thin Kapton foil.

The proton bunch duration was estimated and monitored during the experiments using a plastic scintillator coupled to a photomultiplier tube (PMT, *R9880U-01, Hamamatsu Photonics, Japan*). It was located close to the Kapton foil at an angle of ~10° with respect to the beam axis, detecting scattered protons. The arrival time of individual protons with respect to the stop signal of the beam chopper was converted to signal amplitude by a Time-to-Amplitude Converter (TAC) and stored in a Multi-Channel Analyzer (MCA). The time difference between the proton event and stop signal was chosen to reduce dead time in the TAC. However, this measurement is not sufficiently accurate to obtain reliable sub-ns information on the temporal structure of the proton bunch due to the jitter of the chopper stop signal. It was therefore only used as a diagnostic tool for optimizing the settings of the buncher in order to obtain the shortest possible proton bunches, as well

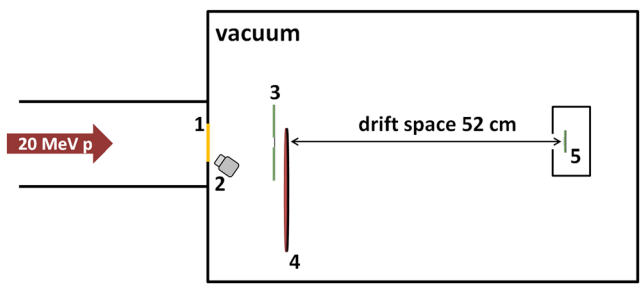

FIG. 3. Schematic overview of the experimental setup. The ns-short, 20 MeV proton bunches are entering from the left, passing through a 50 μm thin Kapton foil (1). A plastic scintillator coupled to a photomultiplier tube (2) detects large-angle scattered protons from the foil. The protons pass a 10 μm thin planar silicon detector (3), a motorized wheel with different absorbers mounted (4), and drift 52 cm through vacuum until they reach the BridgeV2 TOF detector in an aluminum housing (5).

as to verify that the temporal structure of the bunches remains constant within the experiments.

The proton bunches pass through a 10 μm thin silicon detector and passive energy absorbers, which are further described in the following paragraphs. After a drift length of d = 52 cm, the bunches are detected by the BridgeV2 TOF detector.

2. Passive energy degraders

The monoenergetic, 20 MeV proton bunches were passively degraded using two types of absorbers that were fabricated using the PolyJet 3D printing technique and the rigid transparent photopolymer AR-M2. The first absorbers are different slabs of the 3D printed plastic, ranging from 0.2 to 1.6 mm thickness and producing quasi-monoenergetic proton bunches with an increased energy spread due to straggling.

The second absorber was designed and optimized to produce a polyenergetic proton spectrum that resembles the exponential-like energy distribution from laser acceleration, but starting from a lower energy cutoff of around 13 MeV. It consists of a 1.86 mm thick plastic slab with a matrix of 19 × 21 small pits with convex surfaces, each 1.35 mm deep and spaced by 0.85 mm (Fig. 4). The exponential-like energy distribution is achieved since protons from the initially monoenergetic bunches traverse different absorbing plastic thicknesses.

Despite the specified fine printing resolution of 39 × 61 × 15 μm in the x, y, and z dimensions, rather low printing accuracy had been reported.[25,26] Therefore, the actual proton spectrum slightly deviates from the design energy spectrum.

3. Detectors and electronics

TOF spectrometry of (near-)relativistic and highly intense proton bunches requires fast and radiation-hard detectors. In this study, the so-called bridge microdosimeter (BridgeV2) was used to acquire the TOF signal. This silicon-on-insulator (SOI) detector consists of arrays of cubic 3D SVs with a size of 30 × 30 × 10 μm^3, fabricated on a high resistivity n-SOI active layer of 10 μm thickness and a low resistivity supporting wafer.[27] The total geometric area of silicon is 4.1 × 3.6 mm^2. High charge collection efficiency and a fast response with rise times below 0.5 ns (10%–90%) had been shown previously.[27,28] The methodology described in Sec. II A can be applied to other detector types as well, provided that the detector has fast response and its output current signal scales linearly with the energy deposition inside its SV.

The BridgeV2 detector was mounted on a dual in-line (DIL) package and placed on a dedicated, active preamplifier printed circuit board (PCB). To minimize detector capacitance related delays, a very low input impedance front end preamplifier was used. It delivered 25 mV of output voltage per 1 mA signal current into a 50 Ω load and applied a reverse bias voltage of 7 V to the detector. The output was connected via high-frequency compatible SubMiniature version A (SMA) coaxial cables to a 4 GHz oscilloscope (*LeCroy WaveRunner 640Zi, Teledyne LeCroy, USA*) with a sampling rate of 20 GS/s. For spectrum reconstruction, the signals were downsampled resulting in a sampling time of 0.2 ns.

An additional 10 × 10 mm^2 large planar ultra-thin silicon detector[28] was used upstream to trigger the oscilloscope and to define the start time t_0 of the TOF signal. The total geometrical thickness of its active area was thinned down to 10 μm by chemical wet etching.[29] Thus, this transmission detector is hardly perturbing the initial proton energy since the mean energy loss of 20 MeV protons within the detector is 48 keV, according to MC simulations.

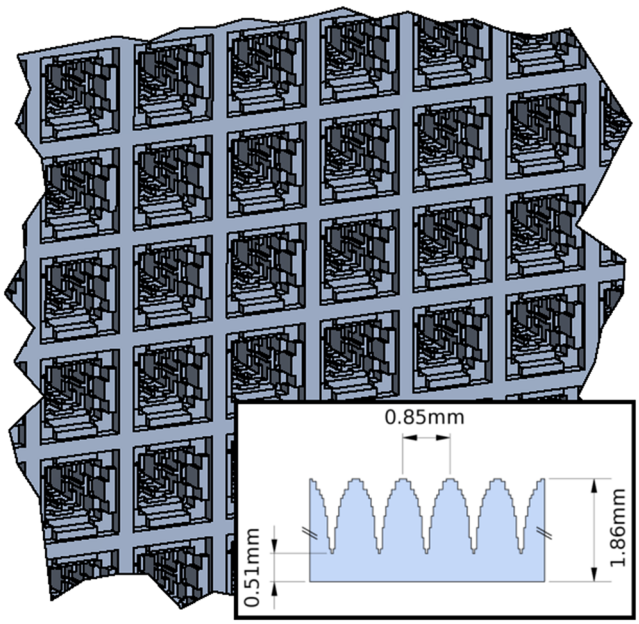

FIG. 4. Excerpt of the CAD drawing of the passive absorber for producing a polyenergetic proton spectrum. The inset shows a 1D-profile through the small pits.

C. Spectrum determination using a magnetic spectrometer

For comparison, the spectra of the proton bunches were measured using a magnetic spectrometer.[30] After the passive energy degraders, the scattered protons are collimated by a 30 μm narrow slit between two 1 cm thick aluminum blocks before they enter a 9 cm long dipole magnet (B = 600 mTesla). Due to the Lorentz force, protons are deflected in the magnetic field perpendicular to the initial beam direction according to their kinetic energy. After a drift space in vacuum of 34 cm, they are detected by the pixelated CMOS detector RadEye.[31] Isoenergy curves were drawn in the detector plane, and with them the signal in each pixel was converted to a proton number according to Lindner *et al.*[30] The slit configuration used in this setup translates to a full acceptance angle of the spectrometer of 6 mrad, resulting in a slight smearing of the signal in the detector plane and hence a broadening of the measured energy spectrum. The additional broadening was compensated by deconvolving the acceptance angle induced spread from the raw signal.

D. FLUKA MC simulations

FLUKA MC simulations were performed to calculate the average energy loss for setting up the system matrix, as well as for a reference to compare to reconstructed energy spectra.

The BridgeV2 detector was modeled in a similar way to the one described in Ref. 32. The initial proton energy distribution from the Tandem accelerator was 20 MeV with an energy spread of 0.1% FWHM. A spot size of the proton beam of 2 mm (FWHM) and a divergence of 5 mrad were used, based on spot size measurements at the experiment using an EBT-3 film.

Since in the experiment the detector was not perfectly aligned on the beam axis, a 2 mm horizontal shift of the detector with respect to the beam axis was also included in the simulation geometry.

III. EXPERIMENTAL RESULTS

A. Measured TOF signals

TOF signals for 20 MeV proton bunches having traversed different absorber thicknesses and the polyenergetic proton bunch are shown in Fig. 5. Since the amplitude of the signals was rather low due to the relatively low proton number per bunch, we averaged over 500 proton bunches. According to simulations and the FC measurements, the average number of protons that actually reached one SV-array of the BridgeV2 detector per bunch was ranging between ~360 and ~3800, depending on the absorber thickness.

The measured TOF signals are clearly separated in time. For the used absorber thicknesses, an increase by 0.2 mm corresponds to energy differences around 0.6–0.7 MeV. The decrease in signal amplitude towards larger absorbers is due to the increased scattering, resulting in a lower particle fluence at the position of the detector. The rising edges of the signal, in which the spectral information of the proton bunches is embedded, clearly differ when comparing the TOF signals of the polyenergetic bunch with a quasi-monoenergetic bunch (the inset in Fig. 5).

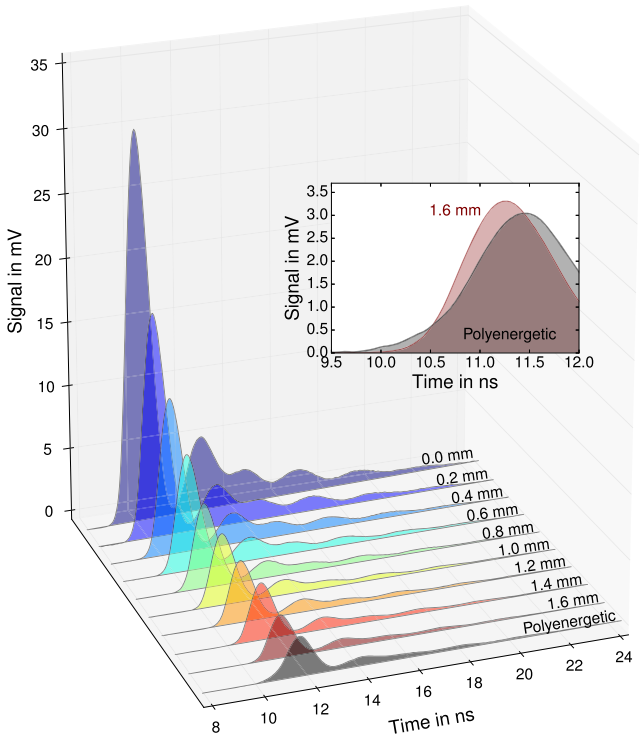

FIG. 5. TOF signals for different absorbers, averaged over 500 proton bunches. The signal corresponding to zero absorber thickness was taken as response R_{meas} to set up the system matrix $\mathcal{A}$ via Eq. (3). The lower signal amplitude for thicker absorbers is due to increased scattering. In the inset, the rising edges of the TOF signal for an absorber thickness of 1.6 mm and for the polyenergetic absorber are magnified and compared.

For each signal curve, only the very first and highest peak actually arises from protons reaching the detector. The undulations encountered in the decaying slopes of all signals originate most likely from parasitic inductance of the detector leads and the DIL socket. Since the TOF signal corresponding to zero absorber was taken as the detector response function R_{meas} which was used to create the normalized detector response R^* via Eq. (3), these oscillations are included in $\mathcal{A}$ and will therefore not affect the spectrum reconstruction.

B. Reconstructed proton energy spectra

Reconstructed proton energy spectra from the TOF signal for a quasi-monoenergetic bunch after an absorber thickness of 1.6 mm and after the polyenergetic absorber are shown in Fig. 6. They are compared to the spectrum expected from FLUKA MC simulations and the measured spectrum using the magnetic spectrometer. For the TOF reconstruction, the regularization parameter in Eq. (2) was set to $\mu = 10^{-6}$, a compromise between numerical broadening of the reconstructed spectrum and overfitting artifacts. The impact of μ is further discussed in Sec. IV A.

From a qualitative point of view, good agreement in the spectral shape is obtained for all three methods. Differences of the reconstructed polyenergetic spectra between simulation and both independent measurements are mainly manifested in the occurrence of two peaks instead of a continuously decaying slope. This can be attributed to the aforementioned low accuracy of the 3D printing process. The deepness of the pits and their convex sides and hence the resulting energy spectrum of the printed absorber differ from its idealized model implemented in the MC simulation.

For the quasi-monoenergetic bunches, the agreement of the mean energy between TOF reconstructed and MC simulated spectrum was better than 2% for every absorber thickness. The energy spread of the reconstructed spectra using the TOF approach is considerably larger compared to the spread calculated by means of MC simulations, but matching quite well the energy spread measured by the magnetic spectrometer.

Also, the absolute numbers of particles measured by the BridgeV2 detector, i.e., the total area under the reconstructed spectra in Fig. 6, are in good agreement with MC simulations taking into account the active area of the detector. Deviations are typically within 5%. Only for three absorber thicknesses used in the experiment, the TOF reconstructed particle number differs by up to 12% from the expected values.

The stability of the spectrum reconstruction was assessed by multiplying the response matrix $\mathcal{A}$ with the reconstructed spectrum, yielding the expected TOF signal for such a spectrum. In Fig. 7, this expected signal is compared to the measured TOF signal for the polyenergetic spectrum. Excellent agreement was found, which indicates that the reconstruction is working properly.

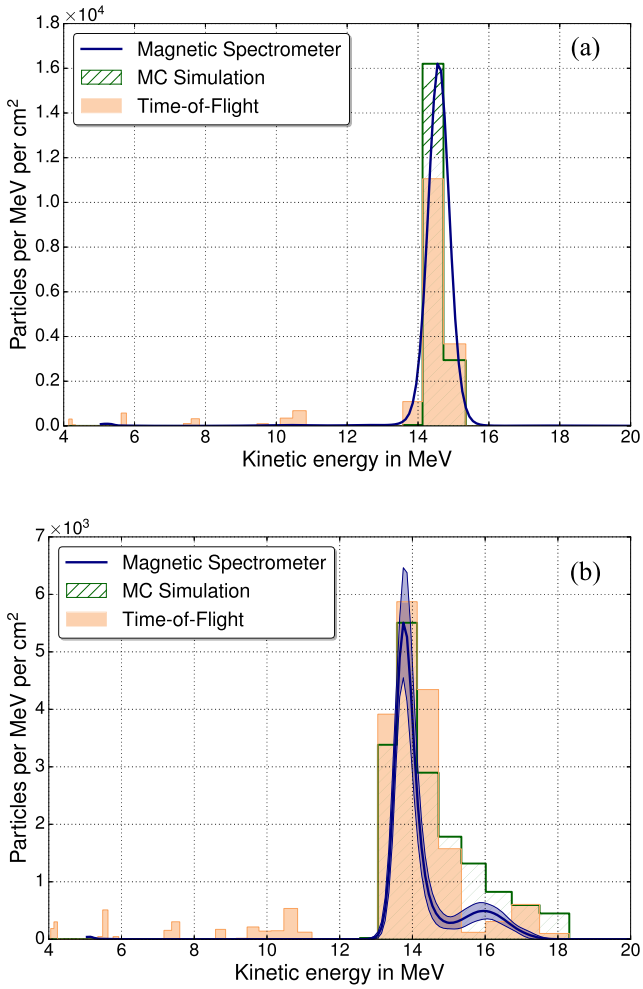

FIG. 6. The reconstructed proton energy spectra (orange) are shown for 1.6 mm plastic absorber (a) and the absorber for polyenergetic bunches (b). For comparison, spectra obtained from MC simulations and measured with the magnetic spectrometer are shown in green and blue, respectively. The bluish area in (b) indicates the encountered spectrum variation depending on the position where the beam spot hits the absorber.

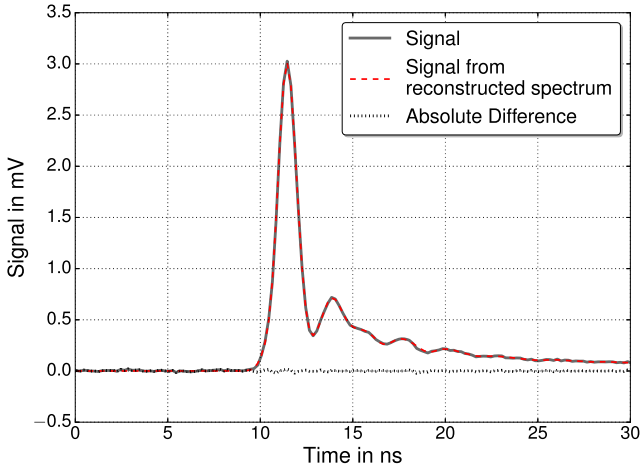

FIG. 7. The measured TOF signal (thick gray line) for the polyenergetic absorber is compared to a signal created by multiplying $\mathcal{A}$ with the reconstructed spectrum (red dashed line). Their absolute difference (dotted black line) is found to be small, indicating a stable reconstruction.

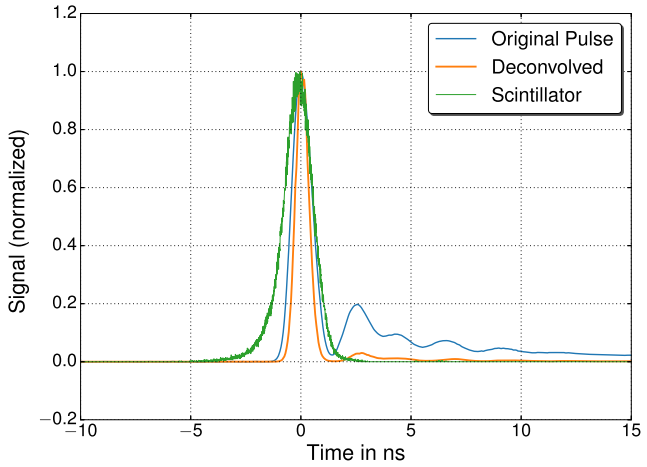

FIG. 8. The temporal pulse structure of the bunched pulses at the Tandem accelerator (orange), obtained by deconvolving the detector response from the measured TOF signal with no absorbers (blue) is compared to the bunch structure determined with the scintillator-based method (green). All curves were normalized with their peaks at $t = 0$, allowing better comparison.

C. Determination of the proton bunch duration

As previously mentioned, the TOF signal acquired with no absorbers is the convolution of the detector response function and the initial temporal structure of the bunched proton beams. Using Richardson-Lucy deconvolution, the proton bunch duration was hence obtained by deconvolving the detector response function, measured with the ultra-short laser pulse, from the TOF signal.

The deconvolved temporal bunch structure and the original TOF signal are shown in Fig. 8, where they are compared to the scintillator-based time measurement. According to a Gaussian fit to the data, the bunch duration is $\tau_{\text{bunch}} = 0.7$ ns (FWHM). It is clearly shorter than the bunch duration measured with the scintillator and the PMT, which was 1.6 ns (FWHM). The reason for this apparently longer bunch duration is due to the jitter of the 5 MHz chopper stop signal. This jitter is in the order of 1–2 ns, which results in a Gaussian smearing of the actual temporal bunch structure, since the method relies on single events from several thousand individual proton bunches.

IV. DISCUSSION

A. Width of the reconstructed energy spectra

In terms of kinetic energy, the reconstructed spectra using our TOF approach are found in good agreement with MC simulations and even better agreement with reconstructed spectra using the magnetic spectrometer. However, differences have been encountered in the energy width of the quasi-monoenergetic proton bunches. These differences can partially be attributed to the use of Tikhonov regularization when solving the least-squares problem. This regularization was used to enhance the smoothness of the reconstructed spectra by penalizing overfitting. Such discontinuities are encountered in the reconstruction of the polyenergetic proton spectrum for a regularization parameter $\mu = 0$.

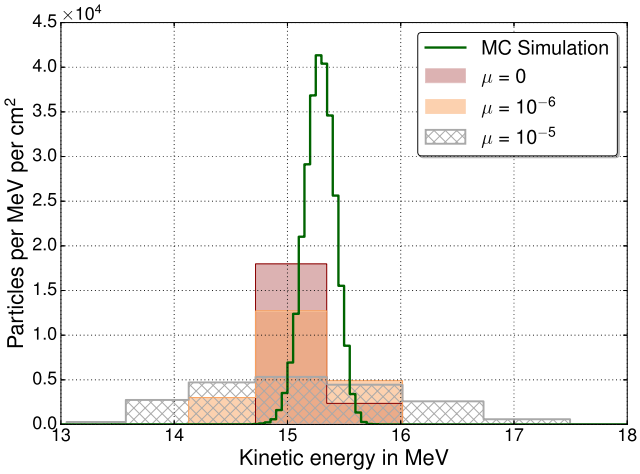

FIG. 9. Width of the reconstructed energy distribution for an absorber thickness of 1.4 mm, depending on the regularization parameter μ. Note that the seemingly large discrepancy between the MC calculated (green) and the reconstructed energy spectrum for $\mu = 0$ (dark red) is only due to the different binning of the data, which was applied for better visibility of the individual histograms.

A comparison of reconstructed spectra for 1.4 mm absorber thickness with different regularization settings is shown in Fig. 9. The impact for different μ can clearly be seen. As the regularization parameter μ should be chosen based on the noise level of the input signal, a characterization study aiming to find appropriate values for μ as a function of the encountered noise is recommended.

For the regularization parameter chosen for the reconstruction of the presented data, the additional broadening remains rather small. This means that the main factor limiting the energy resolution is the temporal bin width itself.

B. Energy resolution

The resolution of the reconstructed spectra presented here is mainly limited by the relatively short drift space of only 52 cm, which was shorter than desirable because of the large beam divergence caused by scattering in the passive absorbers. For an absorber thickness of 1.6 mm, a further increase of drift space from the experimental position to, e.g., 1 m would have resulted in an over 70% lower proton fluence and hence, signal amplitude.

In the case of laser-accelerated particles, low ion fluxes are not a concern anymore and the drift length is only limited by external constraints of the experimental setup. Typical distances between source and the application are in the order of a few metres.[13] Since for a fixed energy range the energy resolution increases approximately linearly with the drift length, resolution may thus be enhanced by around one order of magnitude.

Besides larger drift spaces, an improvement in the energy resolution could potentially be obtained by using faster detectors and high-end readout electronics. When going from the proton energy range in this study (<20 MeV) to energies in the therapeutically relevant range (<250 MeV), time differences corresponding to an energy difference of δE_{kin} = 0.1 MeV decrease by a factor of around 50. Although it is an ambitious task, an energy resolution better than 1 MeV, similar to the resolution presented in this study, could, in principle, also be achieved for proton bunches up to 250 MeV when using a drift space of 5 m and already available detectors[13] and electronics which are 5 times as fast.

C. Uncertainty estimation

The accuracy of the reconstructed energy spectrum is determined by uncertainties related to the timing measurements and the absolute particle number calibration.

The drift time measurement itself is done by the oscilloscope and can be considered fairly accurate. However, inaccuracies may arise from the measurement of the drift length and from the determination of the starting time t_0. For the experiments presented in this study, these uncertainties were estimated to be Δd = 2 mm and Δt_0 = 0.1 ns. For the reconstructed spectra, this adds up to a combined energy uncertainty of 2.4%.

A larger uncertainty was found for the absolute number of protons at the detector. The main reason is the relatively large fluctuation of the beam current during the experiment ($\Delta I/I$ = 25%). Although the data presented here are averaged over 500 individual bunches, current fluctuations on time scales of several seconds are not averaged out. Yet, observation of the signal amplitude measured with the ultra-thin detector suggests a remaining uncertainty below 10%. Also, in the experiments, the BridgeV2 detector was slightly misaligned. The accuracy of the measurement of the alignment with respect to the beam axis was around 0.5 mm. According to MC simulations, this translates into an uncertainty of the actual number of protons on the detector of 6.8%. Combining those uncertainties results in a total uncertainty of the particle number of 12.1%.

In general, these relatively large uncertainties can be easily reduced by longer drift spaces and more accurate length measurements and calibration measurements performed with a more stable proton source.

V. CONCLUSION AND OUTLOOK

We presented an approach for online and absolute spectrometry of ultra-short polyenergetic proton bunches from TOF signals, measured by the sub-ns fast SOI BridgeV2 detector with 10 μm thin SVs and fast readout electronics. Energy distributions are obtained by solving a least-squares problem, accounting for the response function of the detection system.

Validation experiments were performed with passively energy-modulated, ns-short proton bunches from a 12 MV Tandem accelerator in the energy range up to 20 MeV. Within the estimated experimental uncertainties (2.4% and 12.1% for energy and particle number, respectively), reconstructed TOF spectra were found in excellent agreement with MC simulations and measurements using a magnetic spectrometer. Moreover, the temporal pulse duration of the bunched Tandem beam could be indirectly measured by deconvolving the detector response function from the TOF signal of the monoenergetic proton bunch.

The energy resolution was mainly limited by the relatively short drift length, given by experimental constraints. By increasing the drift length and using state-of-the-art electronics, the same resolution as encountered for kinetic

energies around ~20 MeV can, in principle, be obtained for protons in the energy range interesting for proton therapy (<250 MeV).

Within this study, focus was only given to protons, which are typically dominating in laser-ion acceleration. However, such ion bunches may consist of several different ion species and are accompanied by energetic electrons and electromagnetic radiation.[3] The current signal generated by the individual ion species, electrons, and electromagnetic radiation can then be overlapping. Concerning the different ion species, an unambiguous deconvolution without prior knowledge becomes impossible using the presented method. In facilities dedicated to applications of laser-accelerated ions, active beam shaping devices are used to transport the highly divergent ion bunches to the experiment.[6–9] Such devices, e.g., magnetic quadrupoles, are focusing particles of the same species with different kinetic energy to different positions. Setting up a system matrix including various different ion species and penalizing the not-focused energies in the reconstruction algorithm can make it therefore possible to distinguish between the contribution of different ion species, as long as they differ in their charge-to-mass ratio. Such devices will also prevent electrons from reaching the detector, as they are strongly defocused due to their much higher charge-to-mass ratio. On the other hand, detector signal generated by electromagnetic radiation can be deconvoluted from the ion signal by inserting one further copy of the normalized detector response function $R^*(t)$ into the system matrix $\mathcal{A}$. The number of zeros to be inserted to the beginning of the response would then be given by the drift length divided by the speed of light and the sampling time. Thus, the corresponding entry of the vector returned by the least-squares optimization represents the signal generated by electromagnetic radiation.

Moreover, effort is currently ongoing in developing a pixelized detector providing fast timing properties and with a removed support wafer. That way, this detector could then be operated in transmission prior to any kind of application as an online beam monitoring device with almost negligible perturbation of the laser-accelerated ion bunches.

ACKNOWLEDGMENTS

This work has been supported by DFG Cluster of Excellence MAP (Munich-Centre for Advanced Photonics). M. Würl acknowledges financial support from the IMPRS-APS, and F. H. Lindner acknowledges funding by BMBF under Contract No. 05P15WMEN9. Furthermore, we would like to acknowledge support by the Australian Research Council Discovery Project Grant No. DP170102273 (development of microdosimetry detectors). The authors would like to thank G. Dollinger, H. Jakob, J. Gebhard, C. Lenz, M. Pelzer, M. Speicher, and M. Wiesheu for their support related to the experiments.

[1] J. Schreiber, P. R. Bolton, and K. Parodi, Rev. Sci. Instrum. **87**, 071101 (2016).
[2] F. H. Lindner, D. Haffa, J. H. Bin, F. Englbrecht, Y. Gao, J. Gebhard, J. Hartmann, P. Hilz, C. Kreuzer, S. Lehrack, T. M. Ostermayr, T. F. Rösch, M. Speicher, M. Würl, K. Parodi, J. Schreiber, and P. G. Thirolf, in *7th International Conference on Channeling—Charged and Neutral Particles Channeling Phenomena, Sirmione, ITALY, September 25–30, 2016* [Nucl. Instrum. Methods Phys. Res., Sect. B **402**, 354 (2017)].
[3] H. Daido, M. Nishiuchi, and A. S. Pirozhkov, Rep. Prog. Phys. **75**, 056401 (2012).
[4] A. Macchi, M. Borghesi, and M. Passoni, Rev. Mod. Phys. **85**, 751 (2013).
[5] A. Higginson, R. Gray, M. King, R. Dance, S. Williamson, N. Butler, R. Wilson, R. Capdessus, C. Armstrong, J. S. Green, S. J. Hawkes, P. Martin, W. Wei, R. Mirfayzi, X. Yuan, S. Kar, M. Borghesi, R. J. Clarke, D. Neely, and P. Mckenna, Nat. Commun. **9**, 724 (2018).
[6] T. Burris-Mog, K. Harres, F. Nürnberg, S. Busold, M. Bussmann, O. Deppert, G. Hoffmeister, M. Joost, M. Sobiella, A. Tauschwitz, B. Zielbauer, V. Bagnoud, T. Herrmannsdoerfer, M. Roth, and T. E. Cowan, Phys. Rev. Accel. Beams **14**, 121301 (2011).
[7] S. Busold, D. Schumacher, O. Deppert, C. Brabetz, S. Frydrych, F. Kroll, M. Joost, A. Almomani, A. Blazevic, B. Zielbauer, I. Hofmann, V. Bagnoud, T. Cowan, and M. Roth, Phys. Rev. Accel. Beams **16**, 101302 (2013).
[8] T. F. Rösch, P. Hilz, J. Bin, F. Englbrecht, Y. Gao, D. Haffa, J. Hartmann, S. Herr, F. H. Lindner, M. Speicher, M. Würl, K. Parodi, and J. Schreiber, Curr. Dir. Biomed. Eng. **3**, 339 (2017).
[9] A. D. Russo, F. Schillaci, L. Pommarel, F. Romano, A. Amato, A. G. Amico, A. Calanna, G. A. P. Cirrone, M. Costa, G. Cuttone, C. Amato, G. De Luca, F. A. Flacco, G. Gallo, D. Giove, A. Grmek, G. La Rosa, R. Leanza, M. Maggiore, V. Malka, G. Milluzzo, G. Petringa, J. Pipek, V. Scuderi, B. Vauzour, and E. Zappala, in *3rd ELIMED Workshop on Medical and Multidisciplinary Applications of Laser-Driven Ion Beams at Eli-Beamlines, Lab Nazionali Sud, Catania, Italy, September 7–9, 2016* [J. Instrum. **12**, C01031 (2017)].
[10] J. Krasa, A. Lorusso, D. Doria, F. Belloni, V. Nassisi, and K. Rohlena, Plasma Phys. Controlled Fusion **47**, 1339 (2005).
[11] S. Nakamura, Y. Iwashita, A. Noda, T. Shirai, H. Tongu, A. Fukumi, M. Kado, A. Yogo, M. Mori, S. Orimo, K. Ogura, A. Sagisaka, M. Nishiuchi, Y. Hayashi, Z. Li, H. Daido, and Y. Wada, Jpn. J. Appl. Phys., Part 2 **45**, L913 (2006).
[12] M. Cutroneo, P. Musumeci, M. Zimbone, L. Torrisi, F. La Via, D. Margarone, A. Velyhan, J. Ullschmied, and L. Calcagno, J. Mater. Res. **28**, 87 (2013).
[13] S. Busold, D. Schumacher, C. Brabetz, D. Jahn, F. Kroll, O. Deppert, U. Schramm, T. E. Cowan, A. Blazevic, V. Bagnoud, and M. Roth, Sci. Rep. **5**, 12459 (2015).
[14] G. Milluzzo, V. Scuderi, A. Amico, G. Cirrone, G. Cuttone, M. D. Napoli, J. Dostal, G. Larosa, R. Leanza, D. Margarone, G. Petringa, J. Pipek, F. Romano, F. Schillaci, and A. Velyhan, in *3rd ELIMED Workshop on Medical and Multidisciplinary Applications of Laser-Driven Ion Beams at Eli-Beamlines, Lab Nazionali Sud, Catania, Italy, September 7–9, 2016* [J. Instrum. **12**, C03044 (2017)].
[15] D. Margarone, J. Krása, L. Giuffrida, A. Picciotto, L. Torrisi, T. Nowak, P. Musumeci, A. Velyhan, J. Prokůpek, L. Láska, T. Mocek, J. Ullschmied, and B. Rus, J. Appl. Phys. **109**, 103302 (2011).
[16] S. Busold, D. Schumacher, O. Deppert, C. Brabetz, F. Kroll, A. Blazevic, V. Bagnoud, and M. Roth, Phys. Rev. Accel. Beams **17**, 031302 (2014).
[17] V. Scuderi, G. Milluzzo, A. Alejo, A. Amico, N. Booth, G. Cirrone, D. Doria, J. Green, S. Kar, G. Larosa, R. Leanza, D. Margarone, P. McKenna, H. Padda, G. Petringa, J. Pipek, L. Romagnani, F. Romano, F. Schillaci, M. Borghesi, G. Cuttone, and G. Korn, in *3rd ELIMED Workshop on Medical and Multidisciplinary Applications of Laser-Driven Ion Beams at Eli-Beamlines, Lab Nazionali Sud, Catania, Italy, September 7–9, 2016* [J. Instrum. **12**, C03086 (2017)].
[18] A. Ferrari, P. R. Sala, A. Fassó, and J. Ranft, CERN-2005-10 INFN/TC_05/11, SLAC-R-773, 2005.
[19] T. Böhlen, F. Cerutti, M. Chin, A. Fassó, A. Ferrari, P. Ortega, A. Mairani, P. Sala, G. Smirnov, and V. Vlachoudis, Nucl. Data Sheets **120**, 211 (2014).
[20] S. Marrone, D. Cano-Ott, N. Colonna, C. Domingo, F. Gramegna, E. Gonzalez, F. Gunsing, M. Heil, F. Kppeler, P. Mastinu, P. Milazzo, T. Papaevangelou, P. Pavlopoulos, R. Plag, R. Reifarth, G. Tagliente, J. Tain, and K. Wisshak, Nucl. Instrum. Methods Phys. Res., Sect. A **490**, 299 (2002).
[21] F. Belli, B. Esposito, D. Marocco, M. Riva, Y. Kaschuck, and G. Bonheure, Nucl. Instrum. Methods Phys. Res., Sect. A **595**, 512 (2008).
[22] A. N. Tikhonov, Doklady Akademii nauk SSSR **151**, 501 (1963).
[23] W. Assmann, H. Münzer, L. Rohrer, and S. Skorka, Nucl. Instrum. Methods **137**, 19 (1976).
[24] L. Rohrer, H. Jakob, K. Rudolph, and S. Skorka, Nucl. Instrum. Methods Phys. Res., Sect. A **220**, 161 (1984).

[25]K.-i. Kamei, Y. Mashimo, Y. Koyama, C. Fockenberg, M. Nakashima, M. Nakajima, J. Li, and Y. Chen, Biomed. Microdevices **17**, 36 (2015).
[26]S. Waheed, J. M. Cabot, N. P. Macdonald, T. Lewis, R. M. Guijt, B. Paull, and M. C. Breadmore, Lab Chip **16**, 1993 (2016).
[27]L. T. Tran, L. Chartier, D. Bolst, D. A. Prokopovich, S. Guatelli, M. Nancarrow, M. I. Reinhard, M. Petasecca, M. L. F. Lerch, V. L. Pereverlaylo, N. Matsufuji, D. Hinde, M. Dasgupta, A. Stuchbery, M. Jackson, and A. B. Rosenfeld, in *52nd IEEE Nuclear and Space Radiation Effects Conference (NSREC), Boston, MA, July 13–17, 2015* [IEEE Trans. Nucl. Sci. **62**, 3027 (2015)].
[28]M. Würl, S. Reinhardt, A. Rosenfeld, M. Petasecca, M. Lerch, L. Tran, S. Karsch, W. Assmann, J. Schreiber, and K. Parodi, in *Conference on Micro-Mini and Nano-Dosimetry and Innovative Technologies in Radiation Therapy (MMND and ITRO), Tasmania, Australia, January 26–28, 2016* (IOP Publishing Ltd, 2017).
[29]M. Povoli, E. Alagoz, A. Bravin, I. Cornelius, E. Bräuer-Krisch, P. Fournier, T. E. Hansen, A. Kok, M. Lerch, E. Monakhov, J. Morse, M. Petasecca, H. Requardt, A. B. Rosenfeld, D. Röhrich, H. Sandaker, M. Salom, and B. Stugu, J. Instrum. **10**, P11007 (2015).
[30]F. H. Lindner, J. H. Bin, F. Englbrecht, D. Haffa, P. R. Bolton, Y. Gao, J. Hartmann, P. Hilz, C. Kreuzer, T. M. Ostermayr, T. F. Rsch, M. Speicher, K. Parodi, P. G. Thirolf, and J. Schreiber, Rev. Sci. Instrum. **89**, 013301 (2018).
[31]S. Reinhardt, W. Draxinger, J. Schreiber, and W. Assmann, J. Instrum. **8**, P03008 (2013).
[32]L. T. Tran, L. Chartier, D. Bolst, A. Pogossov, S. Guatelli, M. Petasecca, M. L. F. Lerch, D. A. Prokopovich, M. I. Reinhard, B. Clasie, N. Depauw, H. Kooy, J. B. Flanz, A. McNamara, H. Paganetti, C. Beltran, K. Furutani, V. L. Perevertaylo, M. Jackson, and A. B. Rosenfeld, Med. Phys. **44**, 6085 (2017).